Brent L. Weight
Mechanical Eng. Department,
Brigham Young University,
Provo, Utah 84602
e-mail: bweight@et.byu.edu

Christopher A. Mattson
ATL Technology,
Springville, UT 84663
e-mail: mattson@atlconnect.com

Spencer P. Magleby
e-mail: magleby@byu.edu

Larry L. Howell
e-mail: lhowell@et.byu.edu

Mechanical Eng. Department,
Brigham Young University,
Provo, UT 84602

Configuration Selection, Modeling, and Preliminary Testing in Support of Constant Force Electrical Connectors

The recent introduction and advancements in design of simple, constant-force mechanisms have created the potential for small-scale, low-cost, constant-force electronic connectors (CFECs). CFECs differ from traditional connectors by the separation or disassociation of contact normal force and contact deflection. By removing the traditional constraints imposed by forces and deflections that are dependent on each other, new types of electronic connectors can be explored. These new designs may lead to smaller and more reliable electronic connectors. In this paper, constant-force mechanisms are adapted to satisfy current industry practices for the design of electronic connectors. Different CFEC configurations are explored and one is selected, prototyped, and used as a proof-of-concept connector for a personal digital assistant (PDA) docking station. The modeling, optimization, and verification of the prototype CFEC is presented. Adaptation of constant-force technology to electronic connectors creates new possibilities in electronic connector designs, including allowing an optimal contact force to be utilized to decrease the effects of fretting and wear, lowering required manufacturing tolerances, reducing the system's sensitivity to variations introduced by the user, and increasing the system's robustness in applications where movement or vibrations exist.
[DOI: 10.1115/1.2721080]

Introduction

The reliability of high-cycle electronic connectors is of great concern to designers of electronic devices, and methods to improve this reliability are always being evaluated. According to Deshpande and Subbarayan [1], the reliability of high-cycle electronic connectors is related to electrical signal propagation, and mechanical performance and stability. To achieve this reliability in practice, the electronic connectors must transmit the electrical signal with minimal contact resistance under various use conditions and accommodate expected geometric variations in manufacture and assembly. Connector reliability is also partially determined by sliding wear and fretting phenomena [2,3].

The factor that perhaps contributes most significantly to the reliability of electronic connectors is the contact-surface mating conditions. The contact surface finish is critical to maintaining a reliable and noise-free connector. Corrosion on the surface finish can degrade connector performance. Corrosion can be minimized by utilizing a corrosion-resistant material or by designing wipe (the sliding of the two mating surface over each other) into the mechanism. However, wipe can lead to various forms of wear, including adhesive, abrasive, and rider wear. Early researchers [4–6] observed that adhesive wear rates can shift between mild and severe in a very narrow range of load as shown in Fig. 1. This leads to the conclusion that loads at the contact surface should be low enough to prevent severe adhesive wear, yet large enough to maintain minimal contact resistance.

Contact surface finish is also affected by fretting. Antler [2] indicates that during fretting, noise can be introduced into the system due to small amplitude contact movement. He also indicates that even when these movements cease, the wear to the surface from fretting can cause an unacceptably high contact resistance. While factors such as temperature changes and external vibrations that trigger fretting cannot always be eliminated, there are several factors that can decrease the effects of fretting. When fretting can not be eliminated, the effects of fretting can be minimized by minimizing wipe distance and maximizing the contact normal force. However, the maximization of contact normal force will cause adhesive wear as described above if sliding is allowed to occur [2].

Greater reliability can also be achieved when the normal force is consistent regardless of co-planarity differences from adjacent contacts and other geometric variations [7]. Thus a desirable connector system would maintain an optimal contact force regardless of variations due to assembly or use. This optimal force will be in a range were sufficient force is provided to slow the effects of fretting and overcome co-planarity differences in adjacent connectors, but low enough to minimize adhesive and rider wear of the connector system. This optimal force zone is illustrated in Fig. 2.

In addition to achieving high levels of reliability, the electronic connector industry is pushing toward innovative products that fit in smaller packages, have higher contact density, and can support higher data transfer rates. To remain competitive, performance gains must be achieved with designs that can be produced at low cost [8].

The recent introduction and advancements in the design of constant-force mechanisms have created the potential for small-scale, low-cost, constant-force electrical connectors (CFECs). The unique performance characteristics of CFECs differ from traditional cantilever and pogo-type connectors in ways that could lead to new connector applications.

A key performance characteristic of a CFEC is described in Fig. 3. As shown in Fig. 3, a CFEC contact provides a notably smaller change in contact normal force over a sizeable prescribed operational displacement range, when compared to traditional cantilever and pogo-type electrical contacts.

This fundamental characteristic enables the design of connector systems where contact normal force is relatively independent of

Contributed by the Electrical and Electronic Packaging Division of ASME for publication in the Journal of Electronic Packaging. Manuscript received March 21, 2005; final manuscript received July 25, 2006. Review conducted by Bernard Courtois.

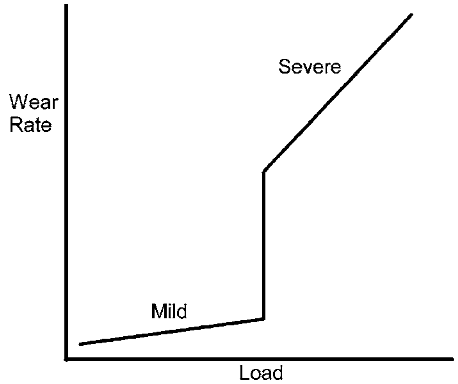

Fig. 1 Effect of load on adhesive wear rates

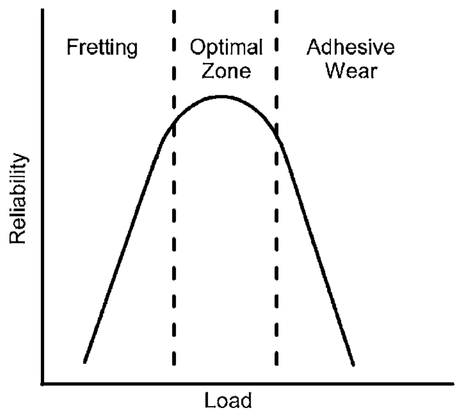

Fig. 2 Depiction of optimal force zone

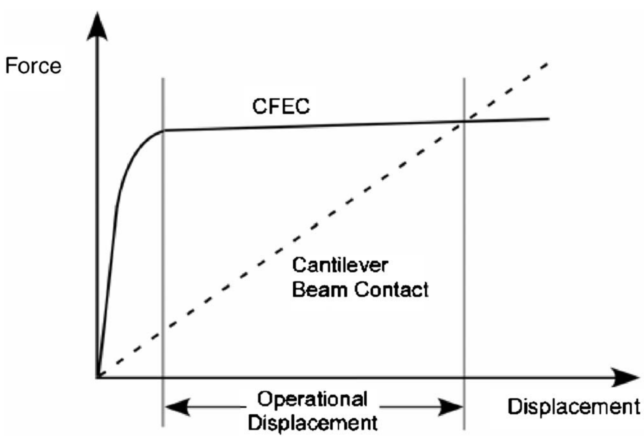

Fig. 3 Force versus displacement curves for a CFEC and a cantilever beam type contact of similar design

contact displacement. Such an independent relationship leads to several potential advantages for CFECs over traditional connectors. Specifically, (i) an optimal contact normal force can be designed and held relatively constant over a large displacement range, thus reducing the effects of fretting without passing the threshold force that triggers sever adhesive wear. (ii) Tolerances for contact-to-contact coplanarity can be loosened while still maintaining small tolerances on normal forces from contact to contact, thus reducing manufacturing stringency without affecting contact performance. (iii) The effects of user-induced variations in connector mating—typically manifest in displacement variation—can be reduced, therefore providing more consistent performance over a large user base. (iv) Improved connection reliability for connector systems exposed to mechanical vibrations, such as those in vehicles, machinery, and computer hard drives, and (v) desired contact normal forces can be achieved with smaller displacements, leading to smaller connector designs.

The force-displacement plot in Fig. 3 also shows a quick initial rise in output force for a CFEC. Although this characteristic is not the focus of this paper, it is worth noting that this quick initial rise can be unseen by the end user through preloading the contact into the prescribed operational displacement range or by simply ensuring that the design displacement is within the operational displacement range.

This paper takes an important step forward in the development of CFECs. Specifically, it presents (i) a brief overview of constant-force mechanism theory as it applies to CFECs, (ii) a connector configuration and model that can be used to apply constant-force mechanism theory to single piece strip-formed electrical contacts, and (iii) a proof-of-concept prototype of one particular constant force electrical connector design that was fabricated, tested, and shown to be a promising step forward in the development of such connectors.

The paper begins by discussing current industry design practices for electronic connectors. It then presents a discussion of constant-force mechanism technology. Different configurations are explored to discover one suitable for application as a CFEC for PDA docking stations. The application is focused on limitations and common industry practices associated with PDA docking stations, but the principles are applicable to a wide range of connector applications. The paper concludes by describing the modeling, optimization, and verification of a CFEC that meets the requirements of the application.

Electronic Connectors

Traditionally, electronic connectors for use in PDA docks have consisted of linear spring assemblies or an arrangement of cantilever beams (see Fig. 4).

Electronic Connector Industry Practices. The electronic connector industry has several practices that constitute essential performance characteristics for electronic connectors. The most basic and important of these are divided into subgroups for presentation here, but it is not intended to be an exhaustive list of all design issues.

The first practice is that the connector provide reliable electrical

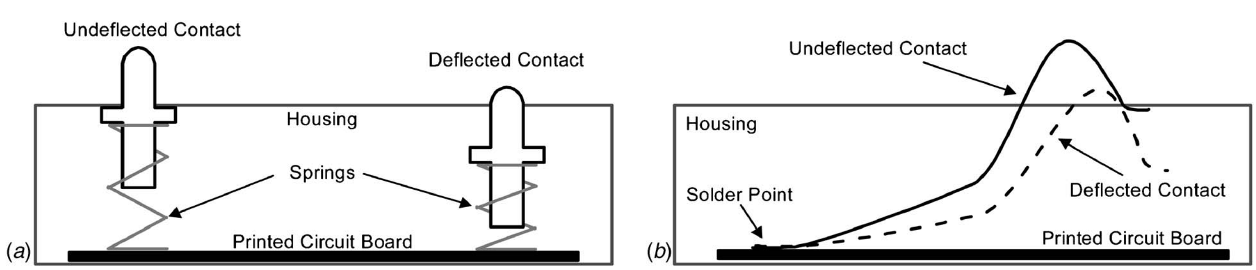

Fig. 4 (*a*) Pogo-type connector and (*b*) cantilever-type connector

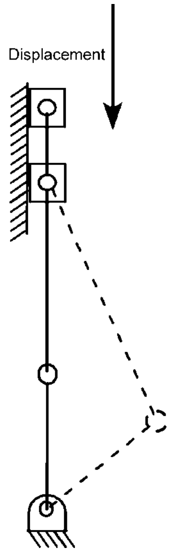

Fig. 5 General compression slider-crank constant-force mechanism

continuity. The electrical path created by an electronic connector can not be interrupted or contain high resistive areas. Additionally, this path should consist of few parts which are easily assembled.

Electronic contacts can be fabricated from any conductive material, but current industry practice is to use alloys that contain copper. Phosphor bronze is a common alloy that is easy to use and readily available. Beryllium copper and titanium copper are commonly used to achieve higher yield strengths. Unfortunately, they are more difficult to use and more expensive than phosphor bronze.

Manufacturability is an important aspect of electronic connector design. Electronic connectors are being produced in ever increasing volumes at lower costs. Current industry practice is to use progressive stamping techniques to shape the metallic beams. Generally, the contacts are stamped at the desired pitch distance and are left attached to the flashing. This allows for easier material handling and assembly, but limits the shape and design of the connector. Some of the limitations imposed on designs due to this manufacturing process are:

- Minimum Material Thickness—There is a minimum material thickness that is suitable for progressive forming
- Minimum Bend Radius—There is a minimum bend radius allowed during stamping operations. A general rule used is four times the thickness of the material

The design of electronic connectors is well defined and understood. However, the examination of cantilever and pogo-type connectors shows that the change in contact normal force over a sizable displacement range is notably larger (steeper slope in the force-displacement plot) than that which is characteristic of a near-constant-force mechanism (see Fig. 3). Therefore, the development of a CFEC requires a new connector configuration to be identified, modeled, and tested. This paper presents a proof-of-concept CFEC configuration, its model, and test results for a prototype connector system.

Constant-Force Mechanisms

Technology Overview. Constant-force mechanisms (CFMs) produce a near-constant output force over a large range of input displacement. This is accomplished by using mechanism geometries and spring constants that produce proportional increases in stored strain energy and mechanical advantage. This proportional increase allows the output force to remain constant throughout the displacement of the mechanism.

For a mechanism configuration to be a candidate for use as a constant-force mechanism, certain key elements must be present. First, a mechanism must have a strain energy storage device. This storage device can take the form of springs or flexible segments. Second, the configuration must allow for an increase in mechanical advantage between the mechanism input and the strain energy storage device.

Once it has been determined that the configuration contains the key elements listed above, optimization is used to determine a mechanism geometry and spring constants that balance the mechanical advantage and the strain energy storage, creating a constant-force mechanism. In this case, the mechanical advantage increases proportionally to allow for more force to be transmitted to the strain energy device as it stores more energy. In this manner, the mechanism input force does not have to increase to achieve additional deflection.

Literature Review. Much effort has been made to design mechanisms that produce a constant output force over a range of input displacements. Nathan [9] proposed a rigid-link constant-force generator. His work resulted in the creation of a hinged lever that produces a constant unidirectional force for any position. This work was extended, resulting in a chain of parallel mechanisms that would support a mass when moved to any position. This mechanism is found in applications such as desk lamp stands. Constant-force tension springs are found in applications such as tape measures and pull starts [10,11]. Jenuwine and Midha [12] proposed a constant-force mechanism that uses rigid links and linear springs to achieve a constant force and has been successfully implemented in concrete testing equipment. Even constant-force control systems have been developed to keep robot and work tool normal forces constant [13,14].

Most recently, compression, slider-crank compliant CFMs have been proposed [15,16], evaluated [17], and improved [18]. Figure 5 illustrates such a mechanism in two positions. Murphy et al. [19] used type synthesis to develop 28 slider-crank configurations that exhibit a near-constant-force while Howell et al. [15] performed dimensional synthesis of several of these configurations. Howell [20] contains design and configuration information for the

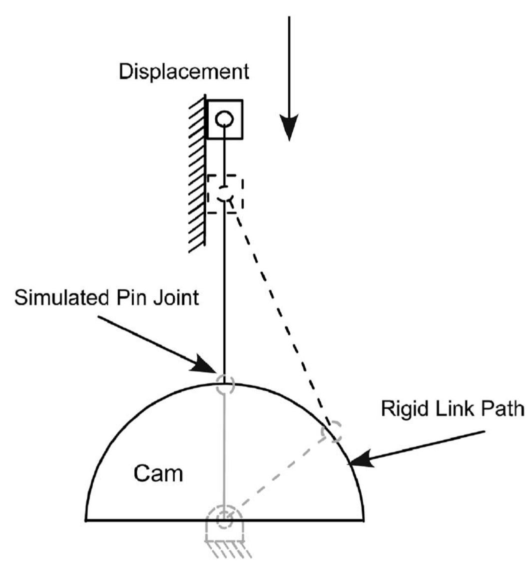

Fig. 6 Simulation of pin joints with a circular cam

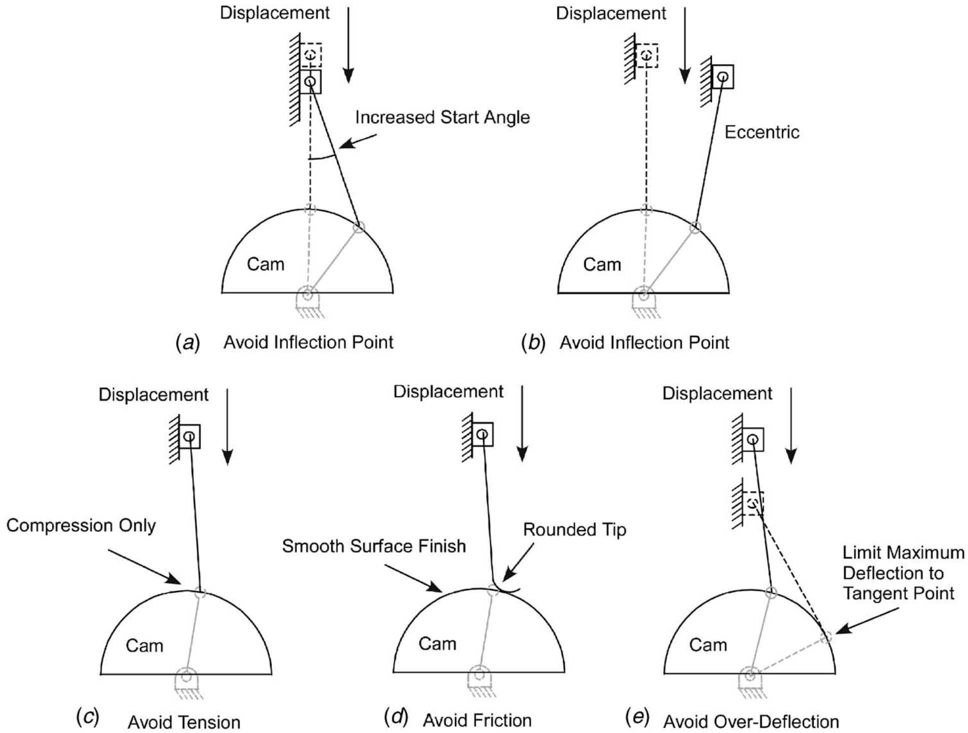

Fig. 7 The above subfigures each illustrate a potential challenge (described in the title) to the simulated pin joint method. Design approaches to address the challenges are described in the subfigure.

slider-crank compliant CFM. Evans and Howell [21] successfully designed and prototyped a constant-force robot end-effector that demonstrated the ability to maintain a constant-force regardless of deflection when coupled with a position-controlled robotic arm.

The latest constant-force mechanism configurations developed are not suitable for use as electronic connectors for several different reasons which include:

- Manufacturability—The stamping of the necessary geometry would be difficult
- Material—The deflections and size constraints would cause extremely high stresses compared to the strengths of common electronic connector materials
- Assembly—The assembly of pin joints makes the use of traditional slider-crank configurations in electronic connectors unlikely
- Electrical Continuity—Pin joints would introduce gaps and areas of high resistance in the electrical path making the connector inefficient and unreliable.

Evaluation of the latest configurations shows that pin joints and small-length flexural pivot cannot be used in electronic connectors, indicating that different configurations must be developed for use as a CFEC.

CFEC Configurations

The development of configurations for use as a CFEC is required. Although traditional electronic connectors and current constant-force mechanisms are not acceptable for use as electronic connectors, they provide a starting point in the search for new configurations suitable for CFECs.

Simulated Pin Joints. The slider-crank constraints can be greatly simplified by using a method that simulates the function and motion of a fixed-pinned flexible segment and a rigid link joined by a pin joint. In this method, a circular cam is used to represent the rigid link. If the simulated joint remains in compression, then the flexible link will follow the cam profile—the exact path of the replaced rigid-body link—as shown in Fig. 6.

However, there are limitations to the simulated pin joint method. Figure 7 provides a graphical summary of the limitations, along with the methods to overcome them. One limitation is that if the flexible beam is loaded, but does not slide around the cam;

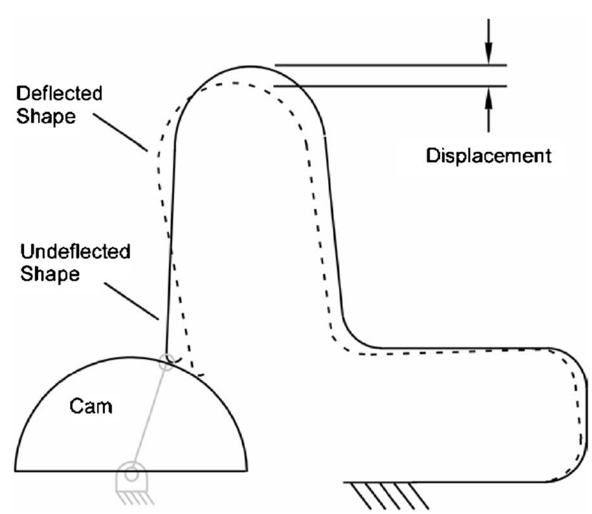

Fig. 8 Selected constant-force electronic connector configuration

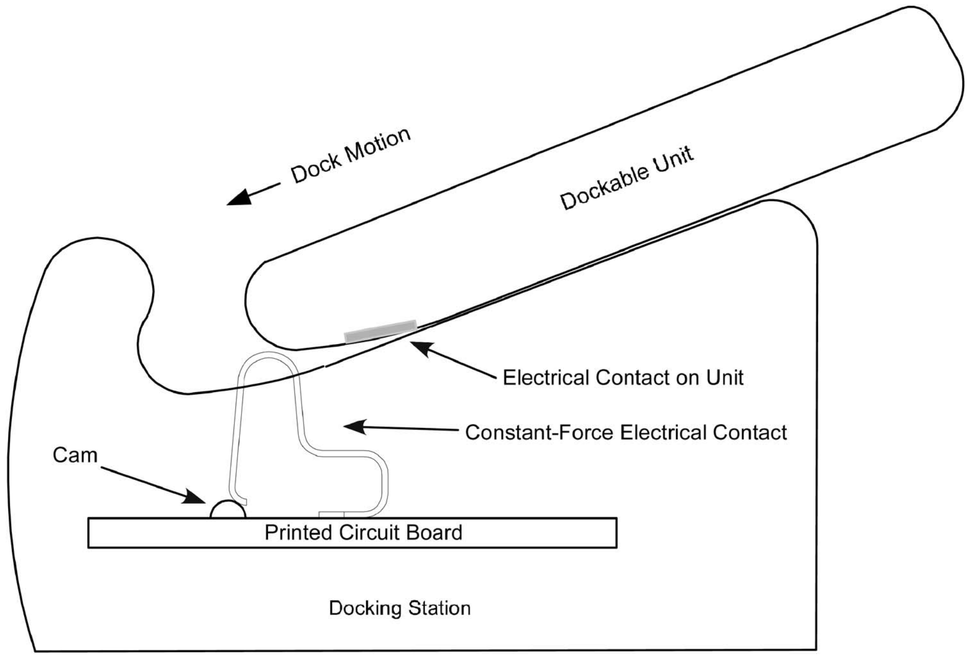

Fig. 9 Selected CFEC configuration in PDA dock

then the beam could buckle. To that end, slider crank change points should be avoided. At these points, it may be difficult to get the beam to begin to slide around the cam. This can be done by changing the initial angle of the beam or changing the eccentricity of the slider crank as illustrated in Figs. 7(*a*) and 7(*b*).

Another limitation is that the contact must be in compression to ensure that the tip of the beam remains in contact with the cam as shown in Fig. 7(*c*). It is also important to ensure that the simulated pin joint has minimal friction so that there is smooth motion around the cam. This can be partially accomplished by rounding over the tip of the beam and providing smooth surface finishes on the cam as shown in Fig. 7(*d*).

Finally, as shown in Fig. 7(*e*), there is a limit to how far around the circular cam the flexible link can travel. If the mechanism is deflected to the point that the contact tip no longer contacts the cam (thus changing the effective length of the beam segment),

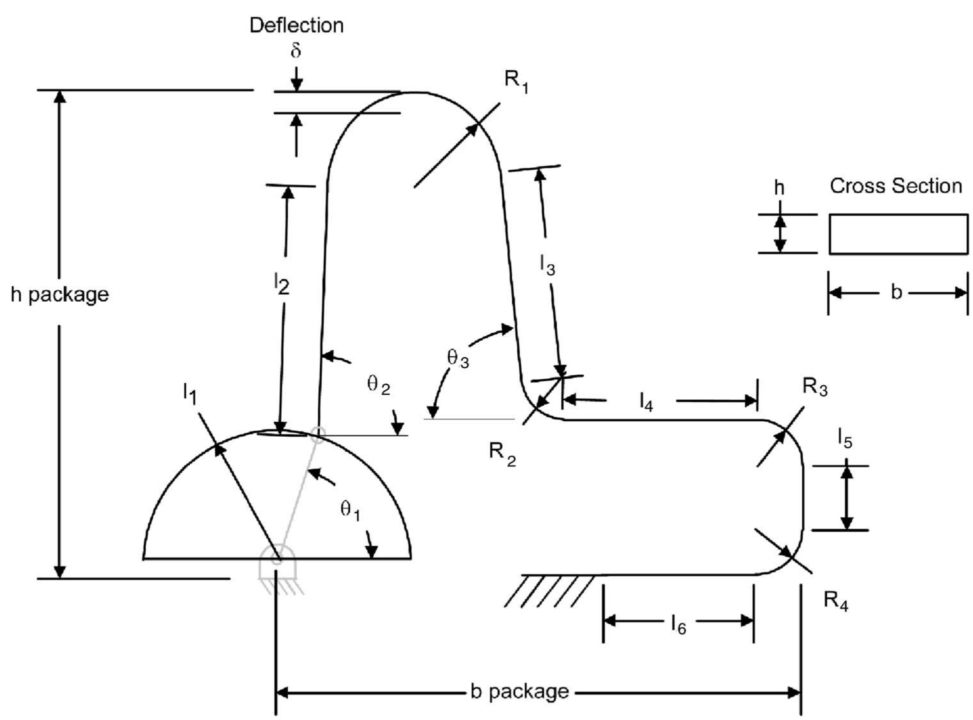

Fig. 10 Important parameters for the selected CFEC configuration

Table 1 Summary of design constraints for prototype CFEC

Description	Model function symbol	General constraint symbol	Constraint value
Connector package height	h_{package}	h_{pc}	≤6 mm
Connector package width	b_{package}	b_{pc}	≤12 mm
Beam cross-sectional height	h	h_c	0.2 mm
Beam cross-sectional width	b	b_c	1.0 mm
Manufacturing bend radius	Bend radius	R_c	≥0.7 mm
Young's modulus	E	E_c	110×10^9 Pa
Material yield strength	Sy	Sy_c	552×10^6 Pa
Design safety factor	SF	SF_c	≥1.0
Connector normal force	Force	$F_{\text{ave},c}$	≈441 mN (45 gf)
Minimum normal force	Minimum force	$F_{\min,c}$	≥294 mN (30 gf)
Maximum normal force	Maximum force	$F_{\max,c}$	≤588 mN (60 gf)
Percent constant force	Percent constant	Ξ_c'	60

then the constant force mechanism will not perform as desired. Despite all of these challenges, the simulation of pin joints with the use of a circular cam is an important tool in the development of a CFEC.

To combine the strengths of constant-force mechanisms and bent-beam electronic connectors, many different possible configurations were evaluated. Using the industry practices criteria and a screening process, the configuration determined most viable for use in a CFEC is one in which a slider-crank mechanism is attached directly to the end of a bent cantilever beam as illustrated in Fig. 8. A concept drawing of the CFEC inside of a PDA dock is shown in Fig. 9.

This configuration is easy to manufacture and assemble, and has electrical continuity. Additionally, the beam and cam combination provide the necessary increases in mechanical advantage and the strain energy storage device necessary for constant-force behavior.

Parameter Definitions. Parameters establish the shape and size of the mechanism and are used as inputs in the model and optimization. Among these parameters are link lengths, angles, and cross-sectional geometries. Some of the parameters are also used to assess performance relative to design requirements associated with the industry practice. A graphical summary of each of the important parameters for the selected configuration is shown in Fig. 10.

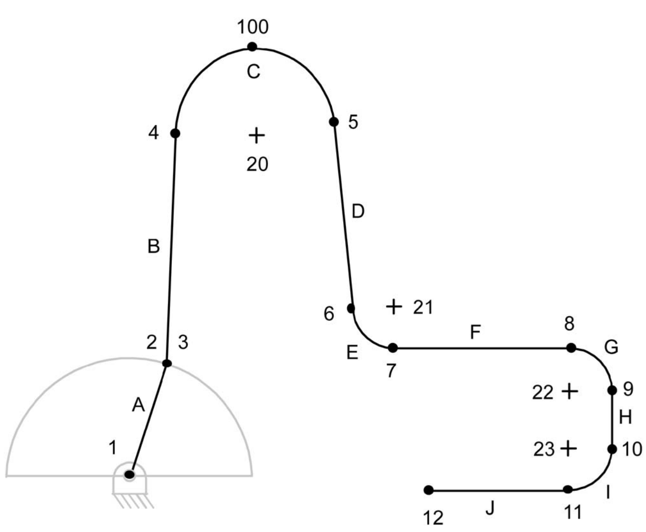

Fig. 11 Key points for the finite element model

Proof-of-Concept Details

The process of moving from the chosen configuration to a commercially viable CFEC is demonstrated by using a specific design application of electronic connectors for personal digital assistants (PDAs) docking stations. Specific requirements for the design application were gathered based on existing dock designs and by working closely with the engineers of a leading manufacturer of these devices.

Although various contact materials could be considered, phosphor bronze, which is perhaps the most common copper alloy used in electronic connectors, is selected for this model. The force range for the design is 294–588 mN (30–60 gf), and the maximum stress in the connector should not exceed the yield strength. The CFEC is required to have a cross-sectional height h of 0.2 mm and a width b of 1 mm. The conditions of the design application also require that the connector fit inside of a 12 mm wide by 6 mm tall rectangle. The final design constraint is that the output force of the mechanism should be at least 60% constant over a large displacement, including the operational displacement, range and most of the preoperational range. The actual force variation through the operational-displacement range is significantly smaller than 40%.

Table 1 summarizes the design constraints for the PDA docking station application. A brief description of each constraint is given in the first column. The symbols for the model functions for each constraint are listed in the second column. The third column contains the general constraint symbol which represents the fixed design constraints for any problems, while the fourth column lists the actual constraint values.

Model Development

It is desirous to produce an accurate model in which the governing parameters can be modified and resulting forces and displacements can be calculated. During the optimization phase, the model is evaluated many times to calculate function values and derivatives. Therefore a simple model is preferred, but it must also be accurate. A finite element analysis (FEA) program capable of nonlinear analysis (ANSYS) was used to model the deflections, contact forces, and stresses in the CFEC. A parametric model was used so that values could be passed between the FEA and optimization programs.

The FEA model was generated using the input parameters to calculate the location of the key points shown in Fig. 11. Once all the key points have been defined, a total of 175 beam elements are used to model the CFEC.

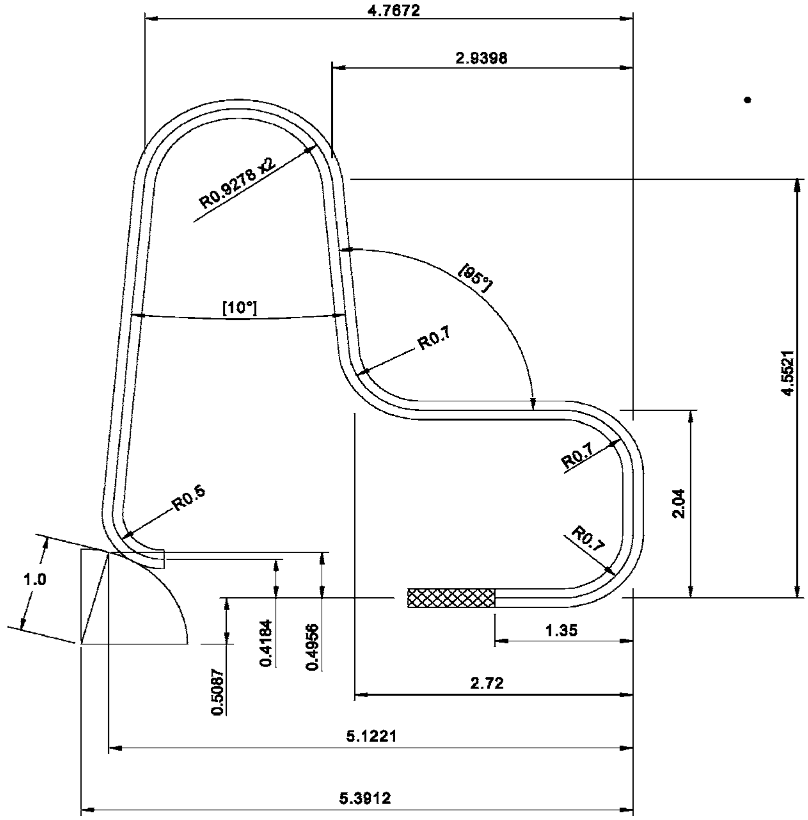

Fig. 12 CFEC proof-of-concept design

The cam is replaced with the rigid link (segment A) that it is simulating. This requires that segment A be pinned to ground at key point 1, and that key points 2 and 3 be constrained to have the same *x* and *y* displacement, thus forming a pin joint. Segment A is given a large width and height to ensure that it is rigid.

It is also necessary to constrain segment J at key point 12 in the *x* and *y* directions, as well as rotation about the *z*-axis. This represents the way the bent beam attaches to ground as a cantilever, simulating its attachment when soldered to a printed circuit board (PCB). Finally, five vertical displacement load steps in the downward direction are applied to the top of the mechanism at key point 100.

Once the model has run for the five different load steps, the contact force for each load step and the highest stresses over the total deflection are written to a data file for use by the optimization software.

Model Optimization

It is necessary to establish an objective function, design variables, design functions, and constraints that facilitate the development of a constant-force mechanism from the layout presented in Fig. 8 and that satisfy all of the design constraints.

The objective function, Ξ', is modeled as 100 times the ratio of the minimum force to maximum force calculated over the mechanism displacement, or

$$\Xi' = 100\frac{\min(\{F\})}{\max(\{F\})} \tag{1}$$

where $\{F\}$ is the force matrix vector containing the output force for each of the five load steps.

If the mechanism has a perfectly constant contact force over the entire displacement, the minimum force will equal the maximum

Table 2 Parameter summary of final design

Description	Model function symbol	Final design	Constraint value
Connector package height	h_{package}	5.9 mm	⩽6 mm
Connector package width	b_{package}	5.4 mm	⩽12 mm
Beam cross-sectional height	h	0.2 mm	0.2 mm
Beam cross-sectional width	b	1.0 mm	1.0 mm
Manufacturing bend radius	Bend radius	0.7 mm	⩾0.7 mm
Young's modulus	E	110×10^9 Pa	110×10^9 Pa
Material yield strength	Sy	552×10^6 Pa	552×10^6 Pa
Design safety factor	SF	1.29	⩾1.0
Connector normal force	Average force	478 mN (48.8 gf)	≈441 mN (45 gf)
Minimum normal force	Minimum force	423 mN (43.2 gf)	⩾294 mN (30 gf)
Maximum normal force	Maximum force	577 mN (58.9 gf)	⩽588 mN (60 gf)
Percent constant force	Percent constant (Ξ')	73.2	60

force and the parameter Ξ' will equal 100. As the two forces become farther apart, the value for Ξ' becomes smaller. This parameter provides a good measure of how constant the output force of the mechanism truly is, and is a natural choice for use as the objective function.

The lengths, angles, and radii described in Fig. 10 are established as design variables (variables changed by the optimization) in the optimization problem with reasonably assumed bounds. The beam height h, width b, modulus of elasticity E, and safety factor (SF) are set up as analytical variables (variables controlled by the user and not affected by the optimization). The values for the analytical variables are established by the design requirements described in Table 1. The remaining constraints are part of the design functions calculated from variables and other model results.

Optimization Problem. Using the design constraints, the optimization problem can be formally stated in as

$$\text{Maximize}\,\Xi' = 100\frac{\min(\{F\})}{\max(\{F\})} \tag{2}$$

Subject to the constraints

$$\Xi' > \Xi'_c \tag{3}$$

$$F_{\text{ave}} > F_{\text{min},c} \tag{4}$$

$$F_{\text{ave}} < F_{\text{max},c} \tag{5}$$

$$SF \geqslant SF_c \tag{6}$$

$$b_{\text{package}} \leqslant b_{pc} \tag{7}$$

$$h_{\text{package}} \leqslant h_{pc} \tag{8}$$

With the following constraints on the design variables:

$$R_1 \geqslant R_c \tag{9}$$

$$R_2 \geqslant R_c \tag{10}$$

$$R_3 \geqslant R_c \tag{11}$$

$$R_4 \geqslant R_c \tag{12}$$

where the variables with a subscript c denote the constraint values found in Table 1.

Optimization and FEA Linking. The optimization was performed using a commercial optimization package. The optimization software generates new values for the design variables and passes them to the FEA code. The model is evaluated for the new design variables, and the results are passed back to the optimization program. This process continues until the reduced gradient optimization algorithm locates a minimum and terminates.

The final design chosen satisfied the design constraints and requirements of the PDA docking station design application. A detailed drawing of the final design chosen for prototyping is shown in Fig. 12. The model values for the design and constraint parameters are listed in Table 2.

Model Validation

To confirm the behavior of the CFEC and the accuracy of the model, nine prototypes of the final design were produced for testing. The photo in Fig. 13 illustrates the comparative size of the prototypes.

Fig. 13 CFEC prototype as compared to a dime

Dimensional Analysis. A dimensional analysis was performed to determine how close the prototypes' dimensions were to the specified dimensions. An optical comparator was used to take 16 dimensional measurements from each of the nine prototypes to determine the variation between the measured values and the design values.

A weighted sum of the variation in each prototype was calculated to determine which of the prototypes were closest to the final design. The connectors closest to the final design were chosen for testing.

Testing. Figure 14 shows a simple representation of the test setup used to test the prototype CFEC. As shown in Fig. 14, a rigid test fixture was designed and used for accurate placement of the prototype. Although the CFEC configuration described in this paper integrates the cam into the connector housing, the cam was fabricated as a separate part for the test setup to allow for different cam materials to be tested, including polypropylene and teflon. The purpose of the different materials was to investigate how different material types affected the performance of the prototype.

A probe and force transducer were attached to a computer-controlled actuator. The computer controlled the actuator and collected position and force data. During testing, the connectors were deflected to 0.75 mm and back.

Results

Nine proof-of-concept prototypes were tested using the test setup described above. Figure 15 shows the force-displacement plot for connector prototype 1 on a polypropylene cam and is

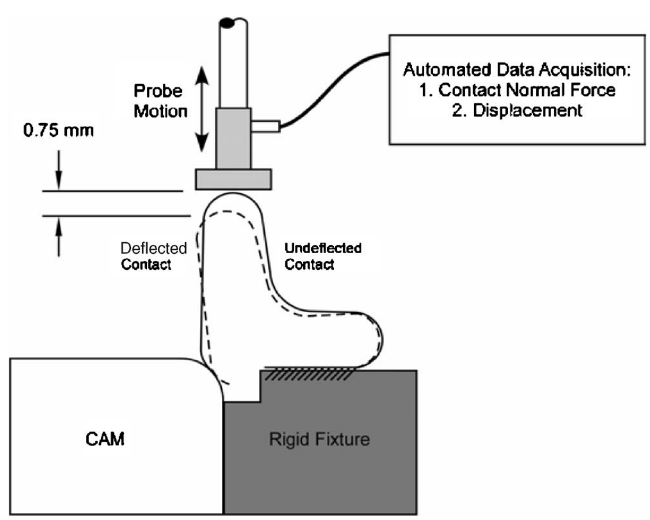

Fig. 14 Schematic of test setup

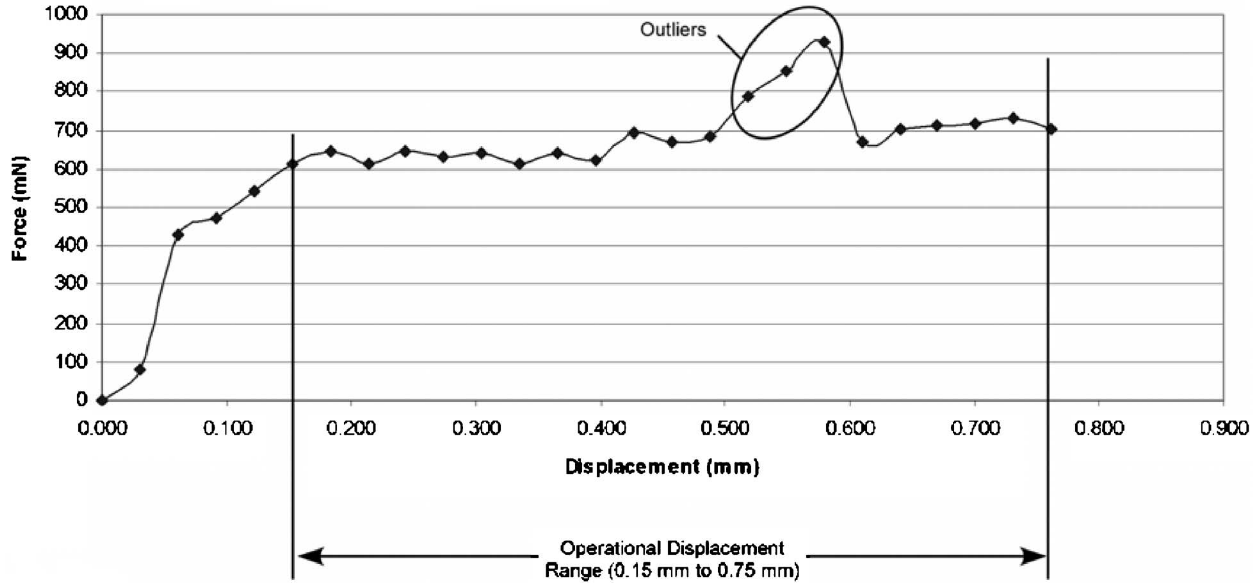

Fig. 15 Graph of force versus displacement from test data

representative of behavior observed for all of the prototypes. Excluding the three outliers circled in Fig. 15, the connector maintains a near constant force in the operational displacement range of 0.15 mm to 0.75 mm. It is important to note that for all of the tests performed, outliers were observed between the 0.5 mm and 0.6 mm deflection range. A surface anomaly is the likely source of the outliers.

As described earlier, CFECs experience a quick initial rise in force in the preoperational displacement range. All nine prototypes tested exhibited this behavior. For the prototyped CFEC design, the quick initial rise was completed within 0.15 mm of displacement. This characteristic was also was observed by Millar et al. [17] during initial testing of constant-force mechanisms. If required, this quick initial rise in force can be unseen by the end user if a deflection preload of 0.15 mm is designed into the connector system. These results provide a promising outlook on the design and manufacturing feasibility of practical CFECs.

A noteworthy phenomenon observed in each of the proof-of-concept test results is described in Fig. 16. The phenomenon is that there is a difference in force between the compression and expansion strokes of the testing. During the compression stroke, the mechanism experienced a higher contact normal force than was predicted. As the mechanism reverses direction, there is a sharp decrease in the force to a point below the predicted force which persists throughout the expansion stroke.

This same phenomenon was also observed by Boyle [22] while studying the dynamics of constant-force mechanisms. In all cases, this behavior is consistent with the effects of friction, which acts in the direction to oppose motion. Boyle [22] was successful at modeling this phenomenon as friction found within the mecha-

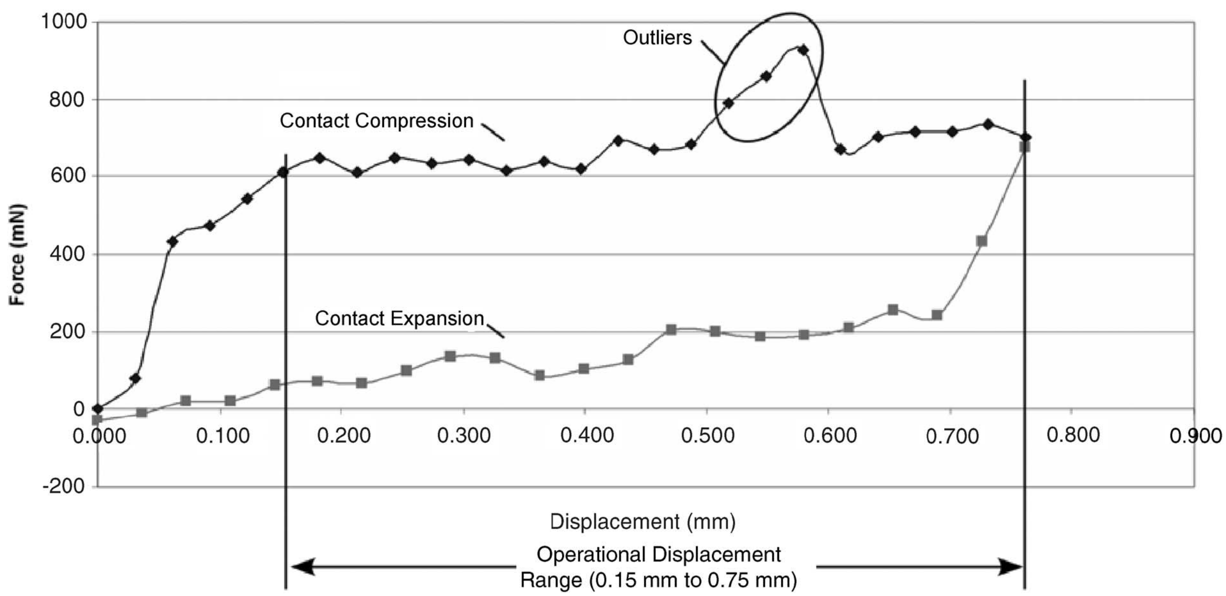

Fig. 16 Graph of force versus displacement during compression and expansion strokes

Table 3 Parameter summary of prototype 1

Description	Function symbol	Prototype 1	Constraint value
Connector package height	h_{package}	5.6 mm	≤6 mm
Connector package width	b_{package}	5.5 mm	≤12 mm
Beam cross-sectional height	h	0.2 mm	0.2 mm
Beam cross-sectional width	b	1.0 mm	1.0 mm
Manufacturing bend radius	Minimum bend radius	0.7 mm	≥0.7 mm
Young's modulus	E	110×10^9 Pa	110×10^9 Pa
Material yield strength	Sy	552×10^6 Pa	552×10^6 Pa
Design safety factor	SF	1.29	≥1.0
Connector normal force	Force	448 mN (45.7 gf)	≈441 mN (45 gf)
Minimum normal force	Minimum force	418 mN (42.6 gf)	≥294 mN (30 gf)
Maximum normal force	Maximum force	500 mN (51.0 gf)	≤588 mN (60 gf)
Percent constant force	Percent constant (Ξ')	79.4	60

nism and testing system. Although a detailed solution to this force difference is beyond the scope of this introductory paper, it is clear that it results from frictional effects and that through minimizing its effect, higher performing CFECs could result.

The accuracy of the model can be verified by comparing the test results with the predicted results. However, the model used for the study does not account for friction, requiring that the effects of the friction be removed from the test data. Assuming that the difference in force between the compression and expansion strokes and the force of the mechanism without friction is the magnitude of the friction force, the effects of friction can be removed by averaging the compression and expansion strokes.

Additionally, to make the comparison between test results and model predictions, new predictions were made based on the actual shape and size of prototype 1. The model parameters and force predictions are listed in Table 3. Figure 17 shows the predicted and average measured forces for prototype 1 with two different cams. The measured forces have been represented, for comparison purposes, without the initial sharp rise in normal force. Importantly, the difference in performance of the polypropylene cam versus the teflon cam is due to the different coefficients of friction belonging to those materials.

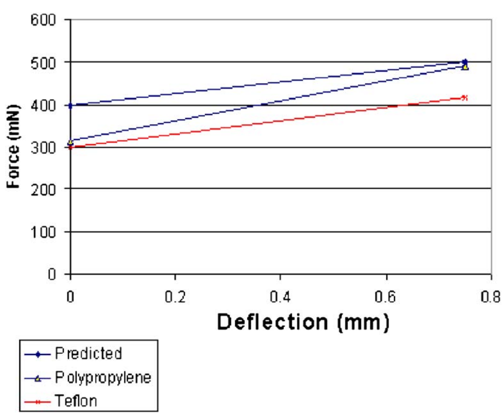

Fig. 17 Average and predicted force comparison for two different cam materials

The percentage of constant-force for prototype 1 can be calculated by using Eq. (1). However, since the model does not include the region of quickly rising forces in the initial deflections, a different method must be used to calculate Ξ'. This is done by taking the lowest average force on the flat part of the curve and the highest force and fitting a line. The parameter Ξ' can then be calculated using the force at the y intercept and the maximum force. This results in a value for Ξ' that is within 12% of the predicted value. Table 4 contains a summary of the comparison between the testing and predicted values.

Conclusions

This paper has taken an important step forward in the development of constant force electronic connectors (CFECs). Specifically, (i) it presents a brief overview of constant-force mechanism theory as it applies to CFECs, (ii) it presents a connector configuration and model that can be used to apply constant-force mechanism theory to single piece strip-formed electrical contacts, and (iii) it presents a proof-of-concept prototype of one particular constant force electrical connector design that was fabricated, tested, and shown to be a promising step forward in the development of such connectors.

The application of constant-force mechanism technology to electronic connectors could provide a number of benefits in terms of performance, reliability, robustness, and package size. Although the design application discussed in this paper requires a contact wiping action and would therefore potentially be subject to conditions of fretting, adhesion ware, and thermal cycling (conditions that are best quantified through stringent experimental testing), the fundamental concept of the CFEC does not require a wiping action.

The successful demonstration of the decoupling of the force and deflection in an electronic connector creates new possibilities in electronic connector designs. These possibilities include allowing a more optimal contact force to be utilized that will decrease the affects of fretting and wear, lowering the required manufacturing tolerances, a reduction of the system's sensitivity to variations introduced by the user, and increased system robustness in applications where movement and/or vibrations exist.

Table 4 Summary of testing and prediction comparisons

	Level of Constant Force		Average force		
	Ξ'	% Error	Force (mN)	Force (gf)	% Error
Predicted	79.42	—	447.97	45.68	
Measured-Teflon® cam	71.89	9.49	402.62	41.06	10.12
Measured-polypropylene cam	63.86	11.17	357.59	36.46	20.17

Acknowledgment

The authors would like to thank ATL Technology for their assistance and expert knowledge in the field of electronic connectors. Additionally, the support of the Utah Center of Excellence for Compliant Mechanisms is appreciated. Special thanks go to Dan Carroll for gathering test data.

References

[1] Deshpande, A., and Subbarayan, G., 2000, "LGA Connectors: An Automated Design Technique for Shrinking Design Space," ASME J. Electron. Packag., **122**, pp. 247–254.
[2] Antler, M., 1999, "Tribology of Electronic Connectors: Contact Sliding Wear, Fretting, and Lubrication," *Electrical Contacts*, P. G. Slade, ed., Marcel Dekker, New York, Chap. 6.
[3] Holm, R., 1999, *Electric Contacts: Theory and Application*, 4th ed., Springer Verlag, New York.
[4] Burwell, J. T., and Strang, C. D., 1952, "On the Emprical Law of Adhesive Wear," J. Appl. Phys., **23**(1), pp. 18–28.
[5] Burwell, J. T., and Strang, C. D., 1952, "Metallic Wear," Proc. R. Soc. London, Ser. A, **212**, pp. 470–477.
[6] Archard, J. F., and Hirst, W., 1956, "The Wear of Metals Under Unlubricated Conditions," Proc. R. Soc. London, Ser. A, **236**, 397–410.
[7] Harper., C. A., 1996, *Electronic Packaging & Interconnection Handbook*, 2nd ed., McGraw-Hill, New York.
[8] Brush Wellman Inc., 1999, *Connector Engineering Design Guide: Material Selection in the Design of Spring Contacts and Interconnections*, Brush Wellman Inc., Cleveland, OH.
[9] Nathan, R. H., 1985, "A Constant Force Generation Mechanism," ASME J. Mech., Transm., Autom. Des., **107**, pp. 508–512.
[10] Wahl, A., 1963, *Mechanical Springs*, 2nd. ed., McGraw-Hill, New York.
[11] Williman, J., 1995, "Small Torque," *Engineering (London)*, Gillard Welch Associates, London, England, pp. 27–28.
[12] Jenuwine, J. G., and Midha, A., 1994, "Synthesis of Single-Input and Multiple-Output Port Mechanisms With Springs for Specified Energy Absorption," ASME J. Mech. Des., **116**(3), pp. 937–943.
[13] Bossert, D., Ly, U. L., and Vagners, J., 1996, "Experimental Evaluation of a Hybrid Position and Force Surface Following Algorithm for Unknown Surfaces," *Proceedings-IEEE International Conference on Robotics and Automation*, IEEE, New York, 3, pp. 2252–2257.
[14] Chang, L. H., and Fu, L. C., 1997, "Nonlinear Adaptive Control of a Flexible Manipulator for Automated Deburring," *Proceedings—IEEE International Conference on Robotics and Automation*, IEEE, New York, Vol. 4, pp. 2844–2849.
[15] Howell, L. L., Midha, A., and Murphy, M. D., 1994, "Dimensional Synthesis of Compliant Constant-Force Slider Mechanisms," *Proc. of DETC'94, ASME Design Engineering Technical Conferences*, ASME, New York, ASME Paper No. DETC98/MEMD-71.
[16] Midha, A., Murphy, M. D., and Howell, L. L., 1995, "Compliant Constant-Force Mechanism and Devices Formed Therein," U.S. Patent 5,649,454, Issued July 22, 1997.
[17] Millar, A. J., Howell, L. L., and Leonard, J. N., 1996, "Design and Evaluation of Compliant Constant-Force Mechanisms," *Proc. of 1996 ASME Design Engineering Technical Conferences and Computers in Engineering Conference*, ASME, New York, ASME Paper No. 96-DETC/MECH-1209.
[18] Weight, B. L., 2001, "Design of Constant-Force Mechanisms," Thesis, Brigham Young University, Provo.
[19] Murphy, M. D., Midha, A., and Howell, L. L., 1994, "Methodology for the Design of Compliant Mechanisms Employing Type Synthesis Techniques With Example," *Proc. of 1994 ASME Mechanisms Conference*, ASME, NDE-Vol. 70, pp. 61–66.
[20] Howell, L. L., 2001, *Compliant Mechanisms*, Wiley, New York.
[21] Evans, M. S., and Howell, L. L., 1999, "Constant-Force End-Effector Mechanism," *Proc. of IASTED International Conference, Robotics & Applications*, Santa Barbara, ACTA Press, Calgary, AB Canada, pp. 250–256.
[22] Boyle, C. L., 2001, "A Closed-Form Dynamic Model of the Compliant Constant-Force Mechanism Using the Pseudo-Rigid-Body Model," M.S. thesis, Brigham Young University, Provo.